

Analytic thermal modeling for dc-to-midrange modulation frequency responses of thin-film high- T_c superconductive edge-transition bolometers

Mehdi Fardmanesh

Thin-film superconductive edge-transition bolometers are modeled with a one-dimensional analytic thermal model with joule heating, film and substrate materials, and the physical interface effects taken into consideration. The results from the model agree well with the experimental results of samples made of large-meander-line $\text{Yba}_2\text{Cu}_3\text{O}_{7-x}$ films on crystalline SrTiO_3 , LaAlO_3 , and MgO substrates up to 100 kHz, the limits of the experimental setup. Compared with the results of the SrTiO_3 substrate samples, the results from the model of the LaAlO_3 and the MgO substrate samples deviate slightly from the measured values at very low modulation frequencies (below ~ 10 Hz). The deviation increases for higher thermal-conductive substrate materials. When the model was used, the substrate absorption and the thermal parameters of the devices could also be investigated. © 2001 Optical Society of America

OCIS codes: 230.0040, 040.3060.

1. Introduction

Responsivity versus modulation frequency and versus the temperature of edge-transition superconductive bolometers has previously been investigated and reported in different studies.¹⁻⁷ Major effects of the substrate-holder and the substrate-film thermal boundary resistances on the response of this kind of bolometer as well as the modulation frequency dependence of the response were reported in previous studies.¹⁻⁷ From the previously reported observations, there have been some efforts to predict the response behavior by use of different thermal models for this type of detector.^{1,3,8-11} These efforts were in particular for the sample types used in this study. In this paper a one-dimensional thermal model and its closed-form solution are proposed for the bolometric response of thin-film high- T_c superconductive edge-transition bolometers on thick crystalline substrates. The proposed model is for dc-to-midrange modulation frequencies above which the limits of the

heat diffusion into the film should also be further considered. The samples considered in this paper carry large-area superconductive patterns compared with the thickness of the substrates.

For the samples with large-area superconducting film patterns compared with the substrate thickness, the thermal boundary resistance at the substrate-holder of the samples, R_{sc} , was found to be considerably higher than that of the other sources such as the film-substrate boundary resistance R_{fs} , the substrate material resistance R_s , and the bulk film thermal resistance R_f .^{1,3,12-14} Hence the total thermal conductance of the device, R_t , was close to the value of R_{sc} , resulting in $R_t \approx R_{sc}$. This is found to be the case at the low-end modulation frequencies.^{3,12} In such a configuration the response of the samples is expected to follow a basic two-lumped-element R - C model. Then R is determined mainly by the thermal boundary resistance at the substrate-holder interface (i.e., R_{sc}), and C is mainly due to the heat capacity of the substrate materials, C_s , which is much higher than that of the film for the considered samples in this paper (i.e., $C \approx C_s \gg C_f$).¹⁵⁻¹⁹ This is reported to be the case up to frequencies at which the thermal diffusion length L into the substrate materials is more than the substrate thickness L_s when the effect of the substrate-cold-finger interface can be seen by the heat wave propagating into the substrate.^{3,12} The increase of the modulation frequency

M. Fardmanesh (fardman@ee.bilkent.edu.tr) is with the Electrical and Electronics Engineering Department, Bilkent University, Ankara 06533, Turkey.

Received 12 June 2000; revised manuscript received 21 August 2000.

0003-6935/01/071080-09\$15.00/0

© 2001 Optical Society of America

Table 1. Dimensions and Thermal Parameters of the Samples Obtained the Proposed Thermal Model^a

| Sample Number | Substrate Material | d^s (cm) | $\left(\frac{C_s}{\text{k cm}^3}\right)$ | $\left(\frac{K_s}{\text{k cm}}\right)$ | $\left(\frac{R_{sc}}{\text{W cm}^2}\right)$ | α | d^f (nm) | A (cm ²) | $\left(\frac{R_{fs}}{\text{W cm}^2}\right)$ | $\left(\frac{C_f}{\text{k cm}^2}\right)$ | $\frac{dR}{dT}$ $\left(\frac{\Omega}{\text{K}}\right)$ |
|---------------|--------------------|------------|--|--|---|----------|------------|------------------------|---|--|--|
| 064-03a | MgO | 0.05 | 0.53 | 3 | 6.82 | 2 | 170 | 0.075 | 4.4 | 642 | 1000 |
| 064-01a | SrTiO ₃ | 0.05 | 0.43 | 0.052 | 5.6 | 1.7 | 220 | 0.017 | 44 | 655 | 1800 |
| 061-02a | LaAlO ₃ | 0.05 | 0.59 | 0.16 | 8.82 | 1 | 550 | 0.075 | 27.5 | 131 | 670 |

^aThe dimensions of the substrates' area are approximately 0.5 cm × 1 cm for all the samples. d_s is the thickness of the substrate, d_f is the thickness of the YBCO film, and R_{sc} is the measured substrate–cold-finger thermal boundary resistance. The factor α is the fitting parameter for the one-dimensional solution obtained from the model. R_{fs} is the film–substrate boundary resistance, and C_f is the heat capacity of the superconducting film obtained from the model. A is the total area enclosed by the superconducting meander-line pattern.

beyond the values at which $L < L_s$ can cause a change in the slope of the response magnitude versus modulation frequency compared with that of the basic R - C model. This was found to happen at a so-called knee frequency f_L , which is dependent on the substrate material and its thickness.^{1,3,12} Considering the thermal diffusion length as the characteristic penetration depth of the temperature variation into the substrate, we can determine the knee frequency from^{3,12}

$$f_L = \frac{D}{\pi L_s^2}, \quad (1)$$

where L_s is the substrate thickness, $D = K_s/C_s$ is the thermal diffusivity of the substrate material, and K_s and C_s are the thermal conductivity and the specific heat (per unit volume) of the substrate materials, respectively.

A different regime of frequency response behavior has been identified based on the above conditions.^{1,3} For frequencies less than f_L , the response was found to scale as f^{-1} following the response for a basic R - C model.^{3,12,15,16} For frequencies higher than f_L , the response was found to scale as $f^{-1/2}$ because of the variation of the effective penetration depth of the temperature variation into the substrate.^{1,3,12} The response follows the $f^{-1/2}$ dependence up to the frequencies at which the thermal resistance of the superconducting film–substrate boundary R_{fs} is negligible compared with the frequency-dependent thermal conductance of the substrate materials R_s . The frequency dependence of the thermal conductance of the substrate R_s can be determined from the thermal diffusion length as

$$R_s = \frac{1}{A\beta\sqrt{C_s K_s \pi f}}, \quad (2)$$

where A is the effective area of the conductive path, f is the modulation frequency in hertz, and β is a correction factor for the above approximation of the effective length of the ac heat flow.^{3,14} The effects of the temperature dependence of the thermal boundary resistance at the substrate interfaces were also found to be partly responsible for the variation of the response versus temperature while still following the basic model at any stable state.¹⁴ Hence the thermal parameters used in the equations should be adjusted for each bias temperature.

There have been different efforts made for response modeling of the edge-transition superconducting bolometers with and without consideration of the effects of thermal boundary resistance at the substrate interfaces and the self-heating or joule heating in the superconducting film.^{1,8,10,11} Based on the above proposed effects of the introduced parameters, successful analyses and predictions have been made of the behavior of the response versus modulation frequency curves of the samples that predict the frequencies at which the slope of the curve changes (the knee frequency).^{1,3} However, they have not predicted and matched the responses in all the measured modulation frequency regimes when an analytic model was used. The present proposed models have predicted and matched the measured responses of the samples at low frequencies, showing different considerable discrepancies at midrange or higher modulation frequencies.^{1,3} To my knowledge, in all the proposed models and solutions, only the magnitude of the response has been considered and compared with the experimental values. This is because the phase of the response was found to be a more sensitive characteristic of the response with respect to the model and the chosen or obtained thermal parameters of the device.¹⁴ In this paper the results obtained from the derived closed-form solution of the proposed one-dimensional model are presented. The results from the model are compared with both the measured values of the magnitude and the phase of the response of the samples.

2. Samples and the Characterization Setup Configurations

The samples studied in this paper were made of 120–550-nm-thick granular superconducting YBa₂Cu₃O_{7-x} (YBCO) films on 0.025- to 0.05-cm-thick crystalline SrTiO₃, LaAlO₃, and MgO substrates. The films were deposited by off-axis planar magnetron sputtering at ~720 °C and patterned by a standard photolithography technique (positive photoresist) modified for less damage to the YBCO material.³ The patterns were made of either a 50- μ m-wide and 1.9-cm-long meander line, giving a total area of 0.017 cm², or a 120- μ m-wide and 4.8-cm-long meander line, giving a total area of 0.075 cm², as listed in Table 1. The resistance versus temperature and the critical temperature T_c of

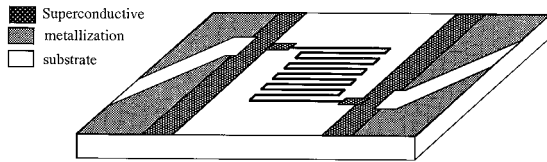


Fig. 1. Typical used superconducting thin film and the electrical contact-area patterns (metallization) of the samples on 1 cm × 0.5 cm area crystalline substrates.

the samples were found to change when the film was exposed to high bias currents or thermal cycling under vacuum, and hence the optimal bias temperature was changed.¹³ The transition temperatures of the samples shifted to lower temperatures because of high bias currents under vacuum and were recovered under a few thermal cycles, reaching a stable value under low bias currents.¹³ Hence the presented data in this paper are obtained with relatively low bias currents under stable conditions and T_c . More details about the fabrication of the samples and their dc characteristics are presented elsewhere.^{3,13,14}

The typical configuration of the studied samples is shown in Fig. 1. The contact areas for the four-probe measurement were coated with either an ~85-nm layer of sputtered gold or an ~60-nm layer of sputtered silver. Electrical contacts to the samples were made with copper wire (32-gauge) and silver epoxy dried at room temperature overnight. To characterize the samples, the second cold stage of a Cryo-Torr 100 was used as the cold finger by a computer-controlled heater. The temperature of the cold finger could be controlled by approximately ±0.1 K from the set points. More details of the characterization setup and the instrumentation are presented elsewhere.^{14,17,20} A sample holder was designed and made of high purity and highly conductive oxygen-free (OFE) copper that was etched in an inert environment gas and coated by a thin layer of gold without being exposed to the atmosphere. The configuration of the holder is shown in Fig. 2.

As shown in Figs. 1 and 2, there are two thermal boundary resistances at the substrate interfaces, one at the film interface and the other at the holder interface. There are two major bulk areas that con-

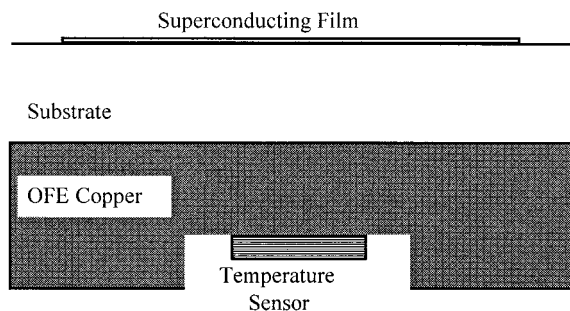


Fig. 2. Configuration of the thin superconducting film samples on a crystalline substrate in contact with the holder and the temperature sensor.

tribute to the overall heat capacity of the samples, one that is due to the superconducting film and one that is due to the substrate materials. Here the OFE copper is considered to be a heat reservoir, the temperature of which is considered uniform at the value measured by the temperature sensor. To obtain a better thermal contact, a very thin layer of either Apiezon-N grease or silicon vacuum grease was used to attach the samples to the holder in the model. The effect of the grease is considered to be included in the measured substrate–holder thermal boundary resistance R_{sc} . The dimensional parameters and the dc electrical and thermal characteristics of interest for the studied samples in this paper are given in Table 1. The given thermal conductivity and the heat capacity of the LaAlO₃ substrate material in Table 1 are obtained by fit of the calculated response versus frequency curve from the model to that obtained experimentally.

The phase and the magnitude of the response versus modulation frequency of the samples, which are the focus of this work, were measured by a lock-in amplifier (EG&G 5406), the input signal of which was amplified by an ultra-low-noise preamplifier (Model 030B, Perry Amplifier). A light-emitting diode (HFE4020, Honeywell) with a peak radiation wavelength of ~0.85 μm was used as the radiation source for the response versus modulation frequency studies in all the measurements. The diode was placed a few centimeters above the sample, providing uniform radiation on the superconducting film pattern. The response of the samples was found to be proportional to the radiation intensity up to 2.13 mW/cm², which was the limit of the source and the radiation intensity for the measurements of the results presented in this paper.

3. Thermal Modeling

From the dimensions given in Table 1 and also as relatively shown in Fig. 2, the area of the superconducting pattern of the samples is large with respect to the substrate thickness. Hence a one-dimensional model is considered and applied for the studied samples in this paper, with all the parameters considered for per unit area. Because of the partial lateral heat diffusion of the heat wave coming from the film into the substrate (the spreading-resistance effect), a correction factor α was obtained for applying to the measured R_{sc} values and is given in Table 1. The value of α was found to increase with the increase of the thermal conductivity of the substrate material and was highest for MgO. It was also found to increase with a decrease in the superconducting pattern area with respect to the substrate thickness, as given in Table 1, and to be higher for the small pattern film on SrTiO₃ compared with that of the LaAlO₃ substrate sample. As given in Table 1, the thicknesses of the superconducting films of the samples were also very small compared with those of the substrate. This allowed the consideration of a lumped-film assumption on the top surface of the substrate in the model.

When the superconducting pattern is considered a

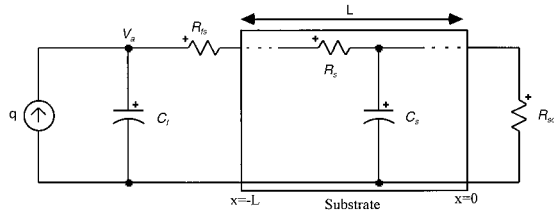


Fig. 3. Equivalent thermophysical diagram of the samples in contact with the cryogenic holder, where q is the input radiation power, C_f is the lumped heat capacitance of the film, C_s and R_s are the heat capacity and the thermal conductivity of the substrate material, respectively, R_{fs} and R_{sc} are the thermal boundary resistance values at the film–substrate and the substrate–holder interfaces, respectively, and V_a is the temperature of the film.

lumped film and the substrate a continuous uniform medium, the thermal equivalent circuit of the samples in contact with the holder can be represented as shown in Fig. 3, where q is the absorbed radiation intensity at the surface of the sample. In this equivalent diagram, two thermal boundary resistances are considered at the substrate interfaces. The heat capacitance of the superconducting film is also considered to be a value representing the total heat capacity of the film per unit area. The thermal conductance of the superconducting film was calculated and found to be negligible compared with that of the substrate and the interfaces. For samples with thicker superconducting films, as for the screen-printed materials,¹⁷ the limited heat conductivity of the superconducting material, which is the same as that for the substrate, should also be considered. Based on the above considerations in the model as shown in Fig. 3, the derivation of the temperature variation and the corresponding thermal parameters for the samples under a constant bias current are presented in the following subsection.

A. Temperature Variation in the Substrate

To approach the complete closed-form solution to the model given in Fig. 3, first we consider the absorbed radiation power q to be applied directly to the surface of the substrate. This is ignoring the effects of the surface boundary conditions of C_f and R_{fs} , which represent the effect of the thermal parameters of the superconducting film at this stage. This particular assumption and the solution to it would be the case for low modulation frequencies. At low modulation frequencies, C_f is much smaller than the contributing heat capacity of the substrate, which can be determined from Eq. (1).³ Also, the film–substrate thermal boundary resistance R_{fs} , is much smaller than that of the substrate–holder or the low-frequency

thermal resistance of the substrate R_s , determined from Eq. (2).

Based on the above assumptions and the steady-state solution to a general one-dimensional heat propagation equation, the temperature variation at the surface of the substrate, ΔT , is obtained. Without consideration of the effect of the superconducting film (i.e., C_f and R_{fs}), ΔT is obtained as follows:

$$\Delta T = q \frac{\exp(\gamma L) + \Gamma \exp(-\gamma L)}{\exp(\gamma L) - \Gamma \exp(-\gamma L)} \left(\frac{1}{j\omega c_s k_s} \right)^{1/2}, \quad (3)$$

where γ is the characteristic thermal impedance of the substrate material defined as

$$\gamma = \frac{1 + j}{(2)^{1/2}} \left(\frac{\omega c_s}{k_s} \right)^{1/2}, \quad (4)$$

$$\Gamma = \frac{R_{sc} - \left(\frac{1}{j\omega c_s k_s} \right)^{1/2}}{R_{sc} + \left(\frac{1}{j\omega c_s k_s} \right)^{1/2}}, \quad (5)$$

where ω is the angular modulation frequency and k_s and c_s are the heat conductivity and the heat capacity of the substrate materials, respectively. The value of R_{sc} can be found from

$$R_{sc} = \frac{1}{G (W/K)/A}, \quad (6)$$

where G is in units of watts per degrees kelvin and is the total thermal conductance of the device at dc or low-end modulation frequencies $G(0)$, and A is the film pattern area. This is based on the assumption that $G_{fs} \gg G_s \gg G_{sc}$, where $G_{fs} = 1/R_{fs}$, G_s is the total heat conductance of the substrate, and $G_{sc} = 1/R_{sc}$. This assumption has been verified for samples with dimensions close to those of our samples, which is discussed in detail and presented elsewhere.^{1,3,12,14,21,22}

B. Temperature Variation at the Film

To find the voltage response to the modulated radiation intensities, the temperature variation in the superconductive film of the samples was obtained for all considered frequency ranges. This temperature variation corresponds to the temperature change across C_f in the equivalent circuit of Fig. 3. Hence the only temperature gradient from the top of the superconducting film into the substrate would be that across the film–substrate interface R_{fs} . When the one-dimensional thermal differential equation is solved with complete boundary conditions, as shown in Fig. 3 (i.e., with consideration of C_f and R_{fs}),

$$\Delta T = q \left[\frac{\frac{\exp(\gamma L) + \Gamma \exp(-\gamma L)}{\exp(\gamma L) - \Gamma \exp(-\gamma L)} \left(\frac{1}{j\omega c_s k_s} \right)^{1/2} + R_{fs}}{\frac{\exp(\gamma L) + \Gamma \exp(-\gamma L)}{\exp(\gamma L) - \Gamma \exp(-\gamma L)} \left(\frac{j\omega}{c_s k_s} \right)^{1/2} C_f + 1 + j\omega C_f R_{fs}} \right], \quad (7)$$

the temperature variation caused by the radiation absorption in the film is found as follows:

where q is the absorbed radiation power in the film per unit area, and C_f and R_{fs} are the total heat capacity of the superconducting film and the thermal boundary resistance at the film–substrate interface per unit area, respectively.

The obtained solution of Eq. (7) is up to frequencies at which the thermal diffusion length into the superconducting film (for YBCO material) becomes smaller or comparable with the thickness of the film. This occurs while the penetration depth or the absorption coefficient length in the superconducting film is still considered to be much smaller than the film thickness. This frequency regime for the samples of Table 1 with a maximum film thickness of ~ 550 nm is found to be much higher than that investigated in this study. As given in Eq. (7), at low frequencies the denominator will approach 1 and R_{fs} will become negligible compared with the first term of the numerator, leading to the results of the one boundary condition problem, as given in Eq. (3). This is because at low modulation frequencies (below ~ 10 Hz in these samples) the temperature variation (heat wave) reaches the bottom of the substrate and hence the heat capacity of the film with respect to that of the whole substrate material under the pattern, and also the thermal boundary resistance at the film–substrate with respect to R_s and R_{sc} becomes negligible.^{3,12}

C. Voltage Response and Bias Current Dependence

Considering a uniform temperature variation in the film, caused by the absorbed radiation ΔT , we can obtain the voltage response in a dc bias configuration from

$$dV = I_b \Delta T \frac{dR}{dT}, \quad (8)$$

where I_b is the dc bias current, dR/dT is the slope of the R versus T curve at the bias temperature as given in Table 1, and ΔT is the temperature variation in the superconducting film as given in Eq. (7). Equation (8) is valid within the temperature variation range within which dR/dT can be considered constant. The maximum temperature variations of the films caused by the radiation were typically below approximately a few millidegrees kelvin, as measured during the characterizations presented in this paper. The transition widths of the samples were typically a few degrees kelvin, and hence the variation of dR/dT or the nonlinearity of Eq. (8) was found to be negligible in the measured and the calculated responses. However, this would not be the case for devices exposed to high radiation intensities that are normally voltage biased for further stability.^{23,24} The effect of the bias configuration on the response and the feedback effect of the joule heating for each case of the voltage-biased and current-biased configurations are discussed and presented elsewhere.¹³

There is also a consecutive temperature variation

that is due to ac joule heating in the film caused by the resistance variation in the superconducting film that is due to the input radiation power. This effect on the response is in the form of positive feedback in the used current-biased configuration as used for the samples in this work. This ac joule heating in a first-order approximation can be considered either as a dependent radiation (or heating) source in parallel to the external radiation source q , as shown in Fig. 3,²⁵ or simply as an additional term in the overall responsivity of the sample as given in the following form^{3,12}

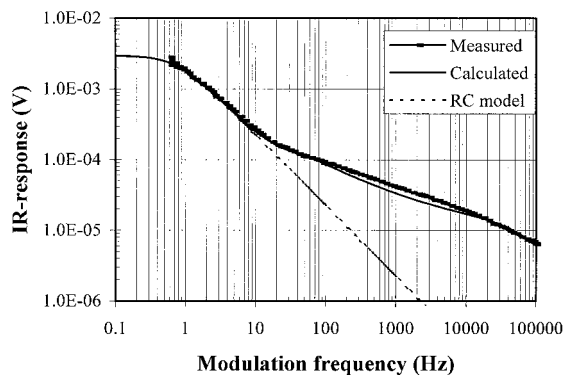
$$r_{v-t} = \frac{r_v}{(1 - I r_v / \eta)}, \quad (9)$$

where r_{v-t} is the overall responsivity in volts per watt and η is the absorption coefficient in the film. When the effect of the absorption coefficient in the q factor in Eq. (7) is considered, r_v will be proportionally related to the dV given in Eq. (8). The effect of ac joule heating in the response of the samples studied in this study is found to be negligible for the used biased currents.

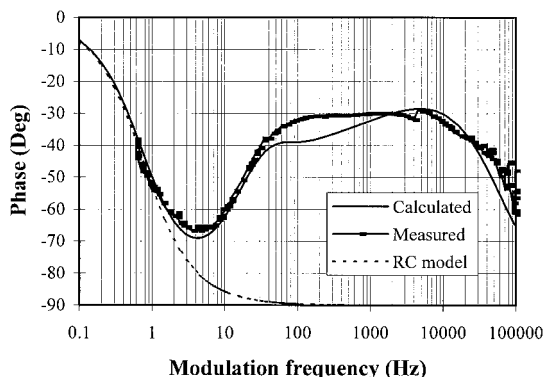
4. Measured Frequency Response and the Results from the Model

The results from the model were compared with the experimental values for the samples given in Table 1. The frequency response behavior of the samples was found to be strongly dependent on the film and the substrate dimensions as well as on the thermal parameters, whereas the observed dependencies were in good agreement with the thermal model. To calculate the response by use of Eq. (7), the dc thermal parameters of R_{fs} , R_{sc} , C_f , C_s , and K_s of the samples were determined. The measured values of the above parameters are given in Table 1. The values of R_{sc} , which are much higher than R_s and R_{fs} , were measured by the method of the resistive or the dc joule heating in the film close to the transition temperature T_c .^{14–16,18} In this method a high bias current is passed through the film and we measure the temperature rise that is due to the joule heating by measuring the resistance of the film. Then, knowing the temperature rise and the joule heating power, we obtain the values of R_{sc} . Parameters such as the film–substrate thermal boundary resistance and the thermal parameters of the substrate or the heat capacity of the samples could also be obtained and verified by use of the fit of the results from the model to the measured values. The values in Table 1 are given per unit area as used in the one-dimensional solution of the model.

The results from the model were investigated for thin-film samples on crystalline SrTiO₃, LaAlO₃, and MgO substrate materials. The measured and the calculated magnitude and phase of the response of the meander-line-patterned YBCO films on the 0.05-cm-thick SrTiO₃, LaAlO₃, and MgO substrate samples are shown in Figs. 4, 5, and 6, respectively. The response calculated with the basic R - C model used in



(a)



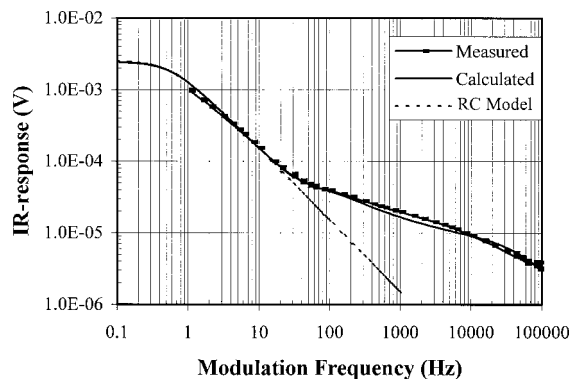
(b)

Fig. 4. Response versus modulation frequency of the SrTiO₃ substrate sample 064-01a at 80 K and 250-mA dc bias current. Measured and calculated (a) magnitude and (b) phase of the response from both the proposed model and the basic *R-C* model.

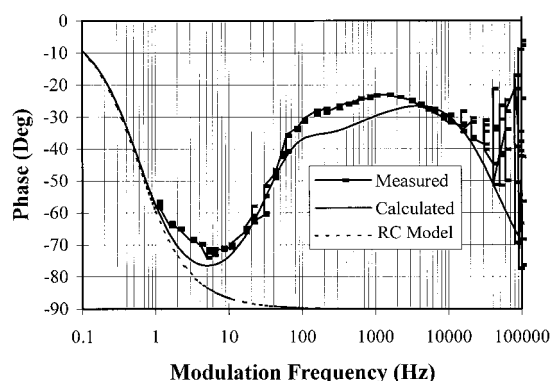
Ref. 3 is also plotted for samples 064-01a and 061-02Aa. The calculated response for the basic *R-C* model is found with

$$r_v = \frac{\eta I}{G + j2\pi f C} \frac{dR}{dT}, \quad (10)$$

where G and C are the total thermal conductance and the heat capacity of the device, respectively. The basic *R-C* model is found to be as useful as the complete model in the low-frequency ranges in which the thermal diffusion length into the substrate is much larger than the substrate thickness. This basic *R-C* model is found to be appropriate for micromachined or freestanding film bolometers. The G and the C values of such bolometers would be constant up to high frequencies at which the thermal diffusion length into the substrate or into the micromachined freestanding base element of the bolometer becomes smaller or comparable with the thickness of the substrate or the base element.^{15,16} In general, the use of the basic *R-C* model is appropriate in the frequency regimes in which one period of the modulation frequency is longer than the low-frequency time response of the samples, τ_L . The τ_L is defined as $\tau_L = C(0)/G(0)$, where $G(0)$ and $C(0)$ are the total low or so-called dc thermal conductance and the heat capac-



(a)



(b)

Fig. 5. Response versus modulation frequency of the LaAlO₃ substrate sample 061-02a at 79.5 K and 500-mA bias current. Measured and calculated (a) magnitude and (b) phase of response from both the proposed model and the basic *R-C* model.

ity of the samples, respectively. In Subsections 4.A–4.C we compare the results from our model with the measured values and investigate the effects of different thermal and dimensional parameters on the fit of the model to the experimental values. The comparison is done for both the magnitude and the phase of the response in three regimes of low, middle, and high ranges of frequencies.

A. Magnitude of Response at Low Frequencies and the Dependence on the Substrate Material and Dimensions

As given in Table 1, the substrate–holder thermal boundary resistances of the samples R_{sc} are given in per unit area and are found by use of the measured dc thermal conductance of the samples by the shift in the temperature caused by joule heating at elevated bias currents.¹⁴ As introduced in Section 3, the factor α was defined for the correction of the R_{sc} value and was found to depend on the area of the pattern A , the substrate thickness d_s , and the thermal conductivity of the substrate materials k_s . It increases by the increase of k_s and the increase of the ratio of d_s/A , as expected. The requirement of the factor α for a better fit of the calculated response curves to the measured ones is interpreted to be due to the spreading thermal resistance effect in the substrate mate-

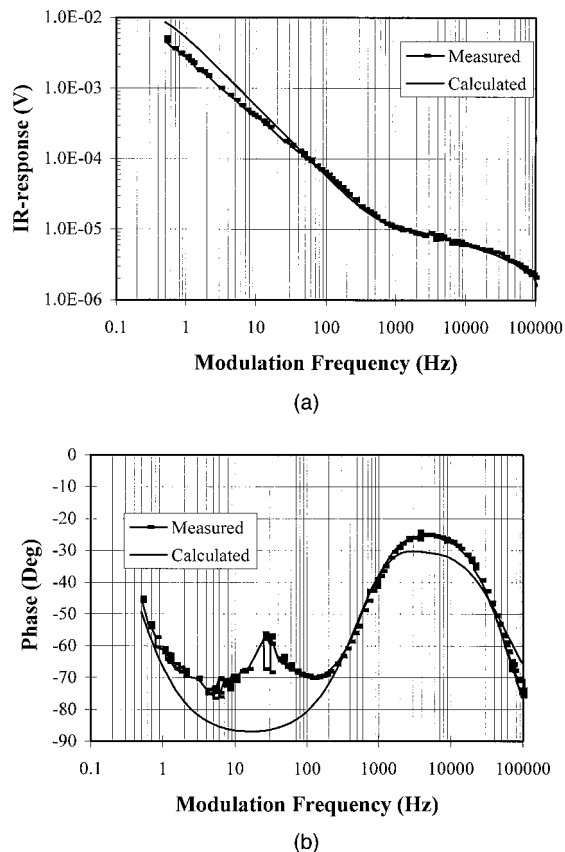


Fig. 6. Response versus modulation frequency of the 0.5-cm-thick MgO substrate sample 064-03a at 79 K and 1-mA bias current. Measured and calculated (a) magnitude and (b) phase of the response.

rial neglected by the one dimensionality of the model. Hence, for a relatively low thermal-conductive substrate sample with a small d_s/A ratio, this factor is expected to approach 1 as obtained for sample 061-02a. By use of the known parameters for the films and the substrates and the obtained values for the α and the boundary resistance, the phase and the magnitude of the response for the samples were calculated and plotted in Figs. 4–6.

As shown in Figs. 4–6, at low modulation frequencies there is a discrepancy between the results from the model and the measured values. This discrepancy was found to increase by the increase of the thermal conductivity of the substrate materials, showing its maximum for the most conductive substrate material. This is also interpreted to be due to the one dimensionality of the model, ignoring the lateral heat diffusion in the substrate materials underneath the pattern. When the magnitudes of the response curves in Figs. 4, 5, and 6, for SrTiO₃, LaAlO₃, and MgO, respectively, are compared, the discrepancy is the most for the most thermal-conductive MgO substrate sample 064-03a of this work. This is also consistent with the variation of α , which is the highest for the same sample. It is proposed that this discrepancy be avoided by use of a three-dimensional solution for the model or use of an

approximate cylindrical solution for a truncated cone structure with a linearly increasing base from the film to the bottom of the substrate. Such approximate solutions can also be applied with simulation programs such as SPICE, in which the parameters can further be considered as frequency dependent.³ The preceding alternative approaches that can be applied to any kind of bolometers are presently under way and will be presented elsewhere.

B. Phase of the Response and the High- and the Low-End-Frequency Behavior

The phase of the response of the samples was found to be much more sensitive to the values of the characteristic parameters of the samples. In particular, the drop of the phase at high-end-frequency response was the determining factor in finding the equivalent values of C_f and R_{fs} given in Table 1. Although the low-end calculated phase of the response is in good agreement with the experimental results for SrTiO₃ and LaAlO₃ substrate samples, there is a peak in the frequency range of 10–100 Hz in the MgO substrate sample that cannot be explained by this model. This behavior was also observed for all other MgO substrate samples. This was found to occur at lower frequencies in thinner substrate samples, e.g., at approximately 10–20-Hz frequencies for 0.025-cm-thick MgO substrate samples compared with those of 0.5-cm-thick MgO substrate sample 064-03a shown in Fig. 6(b). One speculated mechanism for this is interpreted as possibly being due to the reflection and the interference effect of the acoustical phonons within the boundaries of the substrate underneath the superconducting pattern.¹⁴ The possible effect of the superconducting material on the spectral phonon density in the substrate and its consequent effects have already been observed in the phase of the response versus temperature of the samples and are presented and discussed elsewhere.¹⁴

C. Midrange Frequency Behavior of the Phase and the Magnitude of the Response

There is a slight discrepancy in the midrange frequency response curves compared with that of the model. This is clearly seen in the plateau of the phase versus frequency curves for all the samples shown in Figs. 4–6. The discrepancy can also be seen partly in the magnitude of the response curves in the same frequency regime. The measured response in this range was found to be slightly higher in magnitude and more in phase with the radiation signal than the expected values from the model.

The possible effect of the radiation absorption by the open areas of the substrate within the meander lines of the patterns was investigated as a possible source for the discrepancy. This consideration in the model led to a lower phase of the response increasing the observed discrepancy in the plateau region of the phase curves, particularly for the SrTiO₃ substrate sample. The spectral absorption of the crystalline substrate materials was also measured

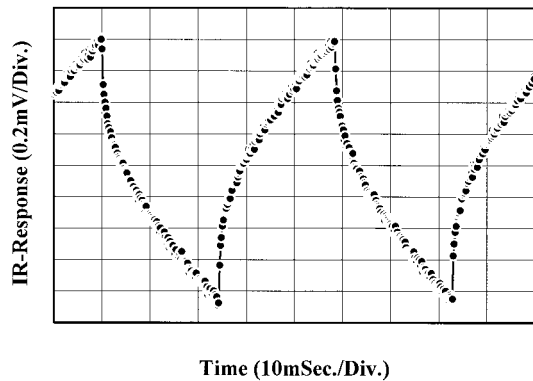


Fig. 7. Steady-state response versus time of SrTiO₃ substrate sample 064-01a at the 560-mA bias current, radiated by a 20-Hz square radiation signal with 2.13-mW/cm² maximum intensity.

from 600 nm to 50 μm and was found to be approximately 12%, 20%, and 8% for the 0.05-cm-thick SrTiO₃, LaAlO₃, and MgO substrates, respectively, at the 850-nm radiation wavelength. Although the effect of the substrate absorption was found to be negligible in the response of the samples measured at the 850-nm radiation wavelength, it was found to have a major effect on the measured spectral response of the samples at longer wavelengths.^{3,7,12,20,26} The effect of the substrate absorption on the spectral response of the detectors in Table 1 was studied and reported elsewhere.^{7,12}

A small and relatively fast component in the time response of the samples was observed and found to increase relatively compared with the total response as the modulation frequency increased. This could not be explained by the thermal response as modeled in this paper. The steady-state time response of SrTiO₃ substrate sample 064-01a in the above-mentioned frequency regime is shown in Fig. 7. As observed from the figure, there exist an abrupt jump and drop at the edge of the on and off switching times of the radiation source. The source is a fast near-IR source that is derived by a square-wave voltage signal, as explained in Section 2. The same type of the steady-state time response is observed for all other samples in the same frequency regime. The effect of this fast component of the response is in favor of the discrepancy (i.e., lowering the phase value and increasing the magnitude of the response from those values calculated by the model). This is interpreted as the nonthermal component of the response and is a possible source for the discrepancy, which needs to be further investigated.

5. Summary and Conclusions

The phase and the magnitude of response versus modulation frequency of superconducting edge-transition bolometers were shown to be strongly a function of the thermal boundary resistance at the film-substrate and the substrate-holder interfaces. A one-dimensional model based on the above facts is proposed for bolometers with superconducting film patterns larger than or comparable with the sub-

strate thickness. The model, while being a useful tool for design optimizations for such devices, could also be used to monitor the thermal parameters of the detectors. The results from the model confirm the major effects of the thermal boundary resistance's dominating the effects of the substrate materials at low- and high-end modulation frequencies. The obtained thermal boundary resistance at the substrate-holder of the studied samples was found to be the limiting factor at the dc or low modulation frequencies.

A good fit between both the measured magnitude and the phase of the response to that obtained from the model could be obtained for the samples from very low modulation frequencies of 0.5 Hz up to ~ 100 kHz, the limits of the setup. The fit matched the best for the SrTiO₃ substrate sample compared with that for the MgO and the LaAlO₃ substrates. From the high-frequency end of the response, the superconducting film-substrate thermal boundary resistance and the heat capacity of the films could be obtained. Both the film-substrate boundary resistance and the superconducting film heat capacity of the samples in this paper were found to be larger than the previously typical reported values in the literature. From the model and from the low and the midrange frequencies of the response, the heat capacity and the thermal conductivity of the used substrate materials (SrTiO₃, MgO, and LaAlO₃) and the substrate-holder thermal boundary resistance could also be obtained. The obtained thermal parameters of the substrate materials agree well with the values previously reported in the literature.

In conclusion, the proposed one-dimensional thermal model can be used to monitor the thermal parameters of the superconducting film, substrate, and the thermal boundary resistance values of an edge-transition superconductive bolometer. Also, the mechanism of heat flow caused by the absorbed radiation in the samples can be investigated by use of the results from the model in this kind of device. The response versus modulation frequency of the bolometers was found to be the most informative data in this respect. The response of the bolometers with large superconducting pattern areas compared with the substrate thickness was found to be mainly bolometric at low and midrange modulation frequencies when following the results from the proposed model. Consideration of a three-dimensional solution to the model would be required for further accurate response analysis of samples with small superconducting pattern areas compared with the substrate thickness.

References

1. P. E. Phelan, "Thermal response of thin-film high- T_c superconductors to modulated irradiation," *J. Therm. Phys. Heat Transfer* **9**, 397-402 (1995).
2. S. Zeuner, W. Prettl, and H. Lengfellner, "Fast thermoelectric response of normal state YBa₂Cu₃O_{7-d} films," *Appl. Phys. Lett.* **66**, 1833-1835 (1995).
3. M. Fardmanesh, A. Rothwarf, and K. J. Scoles, "Low and

- midrange modulation frequency response for YBCO infrared detectors: interface effects on the amplitude and phase," *IEEE Trans. Appl. Supercond.* **5**, 7–13 (1995).
4. M. Nahum, S. Verghese, and P. L. Richards, "Thermal boundary resistance for $\text{YBa}_2\text{Cu}_3\text{O}_{7-x}$ films," *Appl. Phys. Lett.* **59**, 2034–2036 (1991).
 5. A. V. Sergeev, A. D. Semenov, P. Kouminov, V. Trifonov, I. G. Goghize, B. S. Karasik, G. N. Gol'tsman, and E. M. Gershenson, "Transparency of a $\text{YBa}_2\text{Cu}_3\text{O}_7$ -film/substrate interface for thermal phonons measured by means of voltage response to radiation," *Phys. Rev. B* **49**, 9091–9096 (1994).
 6. C. D. Marshal, I. M. Fishman, R. C. Dorfman, C. B. Eom, and M. D. Fayer, "Thermal diffusion, interfacial thermal barrier, and ultrasonic propagation in $\text{YBa}_2\text{Cu}_3\text{O}_{7-x}$ thin films: surface-selective transient-grating experiments," *Phys. Rev. B* **45**, 10009–10021 (1992).
 7. M. Fardmanesh, K. J. Scoles, and A. Rothwarf, "Control of the responsivity and the detectivity of superconductive edge-transition $\text{YBa}_2\text{Cu}_3\text{O}_{7-x}$ bolometers through substrate properties," *Appl. Opt.* **38**, 4735–4742 (1999).
 8. K. Fushinobu, P. E. Phelan, K. Hijikata, T. Nagasaki, and M. I. Flik, "Thermal analysis of the performance of a high- T_c superconducting bolometer," *J. Heat Transfer* **116**, 275–279 (1994).
 9. A. Frenkel, "Mechanism of nonequilibrium optical response of high-temperature superconductors," *Phys. Rev. B* **48**, 9717–9725 (1993).
 10. H. Neff, "Modeling and optimization of high- T_c superconducting bolometers: the effect of film thickness," *J. Appl. Phys.* **69**, 8375–8379 (1991).
 11. M. I. Flik, P. E. Phelan, and C. L. Tien, "Thermal model for the bolometric response of high- T_c superconducting films to optical pulses," *Cryogenics* **30**, 1118–1128 (1990).
 12. M. Fardmanesh, A. Rothwarf, and K. J. Scoles, "The responsivity and detectivity limits for patterned $\text{YBa}_2\text{Cu}_3\text{O}_{7-x}$ superconductive IR-detectors," in *Proceedings of the Sixth International Superconductive Electronics Conference*, H. Kock and S. Knappe, eds. (Physikaisch-Technische Bundesanstalt, Berlin, 1997), Vol. 3, pp. 399–401.
 13. M. Fardmanesh, K. J. Scoles, and A. Rothwarf, "DC characteristics of patterned $\text{YBa}_2\text{Cu}_3\text{O}_{7-x}$ superconducting thin film bolometers: artifacts related to joule heating, ambient pressure, and microstructure," *IEEE Trans. Appl. Supercond.* **8**, 69–78 (1998).
 14. M. Fardmanesh, A. Rothwarf, and K. J. Scoles, " $\text{YBa}_2\text{Cu}_3\text{O}_{7-x}$ infrared bolometers: temperature dependent responsivity and deviations from the dR/dT curve," *J. Appl. Phys.* **77**, 4568–4575 (1995).
 15. A. Jahanzeb, C. M. Travers, Z. Celik-Butler, and D. P. Butler, "A semiconductor YBaCuO microbolometer for room temperature IR imaging," *IEEE Trans. Electron Devices* **44**, 1795–1801 (1997).
 16. C. M. Travers, A. Jahanzeb, D. P. Butler, and Z. Celik-Butler, "Fabrication of semiconducting YBaCuO surface-micromachined bolometer arrays," *J. Microelectromech. Syst.* **6**, 271–276 (1997).
 17. M. Fardmanesh, M. Ihsan, A. Rothwarf, K. Scoles, and K. Pourrezaei, "Thick and thin film Y–Ba–Cu–O infrared detectors," *AIP Conf. Proc.* **251**, 681–691 (1991).
 18. M. Nahum, Q. Hu, P. L. Richards, S. A. Sachtjen, N. Newman, and B. F. Cole, "Fabrication and measurement of high T_c superconducting bolometers," *IEEE Trans. Magn.* **27**, 3081–3084 (1991).
 19. P. L. Richards, J. Clarke, R. Leoni, Ph. Lerch, S. Verghese, M. R. Beasley, T. H. Geballe, R. H. Hammond, P. Rosenthal, and S. R. Spielman, "Feasibility of the high T superconducting bolometer," *Appl. Phys. Lett.* **54**, 283–285 (1989).
 20. M. Fardmanesh, A. Rothwarf, and K. J. Scoles, "Noise characteristics and detectivity of $\text{YBa}_2\text{Cu}_3\text{O}_7$ superconducting bolometers: bias current, frequency, and temperature dependence," *J. Appl. Phys.* **79**, 2006–2011 (1996).
 21. H. Chou, H. Z. Chen, M. T. Hong, Y. C. Chen, and T. C. Chow, "Bolometric detection in a precipitation free $\text{YBa}_2\text{Cu}_3\text{O}_{7-x}$ film at 77 K," *Appl. Phys. Lett.* **68**, 2741–2743 (1996).
 22. J. H. Hao, F. Q. Zhou, X. R. Zhao, H. D. Sun, X. J. Yi, and Z. G. Li, "Responsivity calculation and measurement of YBaCuO optical detector," *IEEE Trans. Appl. Supercond.* **3**, 2167–2169 (1993).
 23. G. D. Poulin, J. Lachapelle, S. H. Moffat, F. A. Hegmann, and J. S. Preston, "Current-voltage characteristics of dc voltage biased high temperature superconducting microbridges," *Appl. Phys. Lett.* **66**, 2576–2578 (1995).
 24. K. D. Irwin, G. C. Hilton, D. A. Wollman, and J. M. Martinis, "X-ray detection using a superconducting transition-edge sensor microcalorimeter with electrothermal feedback," *Appl. Phys. Lett.* **69**, 1945–1947 (1996).
 25. Z. M. Zhang and A. Frenkel, "Thermal and nonequilibrium responses of superconductors for radiation detectors," *J. Supercond.* **7**, 871–883 (1994).
 26. K. Kamaras, K. L. Barth, F. Keilmann, R. Henn, M. Reedyk, C. Thomsen, M. Cardona, J. Kircher, P. L. Richards, and J. L. Stehle, "The low-temperature infrared optical functions of SrTiO determined by reflectance spectroscopy and spectroscopic ellipsometry," *J. Appl. Phys.* **78**, 1235–1240 (1995).